Study on a novel poly (vinyl alcohol)/graphene oxide-citicoline sodium-lanthanum wound dressing: Biocompatibility, bioactivity, antimicrobial activity, and wound healing effect

Liu, Yihan; Zhang, Qicheng; Zhou, Ninglin; Tan, Jingting; Ashley, Jon; Wang, Wentao; Wu, Fan; Shen, Jian; Zhang, Ming

Published in:
Chemical Engineering Journal

Link to article, DOI:
10.1016/j.cej.2020.125059

Publication date:
2020

Document Version
Peer reviewed version

Study on a Novel Poly (vinyl alcohol)/Graphene Oxide-Citicoline Sodium-Lanthanum Wound Dressing: Biocompatibility, Bioactivity, Antimicrobial Activity, and Wound Healing Effect

Yihan Liu[a+], Qicheng Zhang[a+], Ninglin Zhou[a*], Jingting Tan[a], Jon Ashley[b], Wentao Wang[a,b*], Fan Wu[a], Jian Shen[a], Ming Zhang[a*]

[a]*Jiangsu Collaborative Innovation Center for Biomedical Functional Materials, School of Chemistry and Materials Science, Nanjing Normal University, Nanjing 210023, China;*

[b]*Department of Health Technology, Technical University of Denmark, Kongens Lyngby, 2800, Denmark;*

Corresponding authors: Wentao Wang, wentwa@dtu.dk; Ming Zhang, 151102067@stu.njnu.edu.cn; Ninglin Zhou, zhouninglin@njnu.edu.cn.

+These authors are equal contribution.

Abstract

Although graphene oxide (GO) is widely used as an antibacterial agent, its efficacy still needs to be improved. In this work, we present a novel medical dressing that improves antibacterial effect and promotes wound healing. Poly (vinyl alcohol)/graphene oxide-citicoline sodium-lanthanum (PVA/GO-CDPC-La) films were prepared by the solution intercalation method for usage in wound dressing applications. GO was modified by zwitterionic citicoline (CDPC) to improve the dispersibility of water-based polymers, while providing La^{3+} ions with more adsorption sites and enhancing the antibacterial properties of the film. Water absorption experiments showed that it could effectively absorb wound exudate while keeping the wound moist.

In vitro cytotoxicity and cell adhesion experiments showed that the PVA/GO-CDPC-La films had good biocompatible and promoted wound healing. Bacterial adhesion experiments showed PVA/GO-CDPC-La could greatly reduce the risk of wound infection. Furthermore, *in vivo* wound healing experiments showed that wounds treated with the film healed faster postoperatively and histological observations showed that a mature epidermal architecture was formed, which could be used as a wound-dressing material.

Keywords: graphene oxide; citicoline; lanthanum; wound healing; antibacterial.

1. Introduction

Skin is the largest organ in the human body. It covers the whole body surface and is an important shield to maintain the stability and prevent the invasion of external pathogens [1-3]. If the skin has the serious damage, it can cause many local and systemic problems, such as acceleration of metabolism, evaporation loss of moisture, protein and immune system disorders, pathogens such as bacteria and fungi will take the opportunity to breed in the wound and cause infection, giving rise to various complications and serious life-threatening infections [4]. Reconstruction or protection of the protective shield of skin is the ultimate goal of empyrosis, cuts, abrasions, and skin ulcers. Medical dressings can replace some parts of the protective function of damaged skin temporarily, provide a suitable environment for wound healing, and play an important role in helping restore skin tissue and function [5,6]. The ideal medical dressing needs to provide a moist environment for the wound surface, absorb the tissue fluid and blood from the wound quickly to keep the wound clean. In addition, it should

have the ability to inhibit bacteria, microbial penetration, reproduction, and reduce the risk of infection [7-9]. Early cotton and linen based medical dressings only have a simple wound protection functionality, as they cannot provide a closed and moist environments, so they easily adhere to the wound, and improper replacement can easily cause secondary damage. It is difficult to achieve a good therapeutic effect on severe large-area traumas. At present, closed and semi-closed polymer dressings that keep wounds moist have become the mainstream in the development of medical dressings [10].

Polyvinyl alcohol (PVA) is a water-soluble high molecular weight polymer obtained by polymerization and alcoholysis of vinyl acetate under acid or base catalysis [11]. Due to its ease of synthesis, good chemical blocking and biocompatibility, PVA has become an extensively applied polymer that can be used in fiber textiles, food packaging, construction, agriculture, and biomedical materials, etc. [12,13]. Films, hydrogels, and fiber textiles prepared from PVA have considerable potential as medical dressings [14-16]. However, most of the dressing materials prepared from PVA lack one or properties such as lower mechanical properties, insufficient blood clotting ability, lower swelling capacity, and inadequate antibacterial activity [17]. Recently, it has been demonstrated that the oxygen-containing groups in graphene oxide (GO) form strong hydrogen bonds with the PVA chain and thus can be uniformly dispersed and completely detach from the PVA matrix [18,19].

Citicoline (Cytidine-5’-diphosphocholine) is an important mononucleotide, and is also an endogenous nucleotide found in the human body [20]. Its basic structure is

divided into two parts: cytidine and choline. Experiments have shown that citicoline can participate in the repair and regeneration of central nervous systems. It can also prevent and protect neural cell membrane damage [21,22]. In recent years, ammonium phosphate zwitterions with a cell-like structure membranes have attracted the attention as biomaterials for researchers. A large number of studies have focused on the use of ammonium phosphate zwitterions as raw materials to construct a surface with superior biocompatibility [23]. Since one end of the citicoline molecule has a choline part, which is similar to the ammonium phosphate zwitterion, its modification on the surface of a material (such as GO, polymer, and black phosphorus, etc.) can regulate hydrophilicity, blood compatibility, and histocompatibility of the material effectively [24].

Over the last few decades, due to increased drug resistance, antibacterial agents commonly used in the market are becoming increasingly important with many researchers beginning to focus on the use of rare earth elements such as Lanthanum (La^{3+}) containing compounds, with the hope to use them as new and effective antibacterial substances [25,26]. La^{3+} and its compounds have the advantage of possessing comparable anti-bacterial properties, broad-spectrum properties, low toxicity, and low doses required [27]. It is expected to be a new type of antibacterial agent and used to prepare anti-infection antibacterial materials. At present, the antibacterial mechanism of La^{3+} has been confirmed by articles [28,29]. La^{3+} changes the conformation of peptidoglycan or teichoic acid by coordinating with the carboxyl and carbonyl of peptidoglycan in the bacterial cell wall, or phosphorus-oxygen bonds in teichoic acid, causing cell wall voids and leads to leakage of inclusion [30,31].

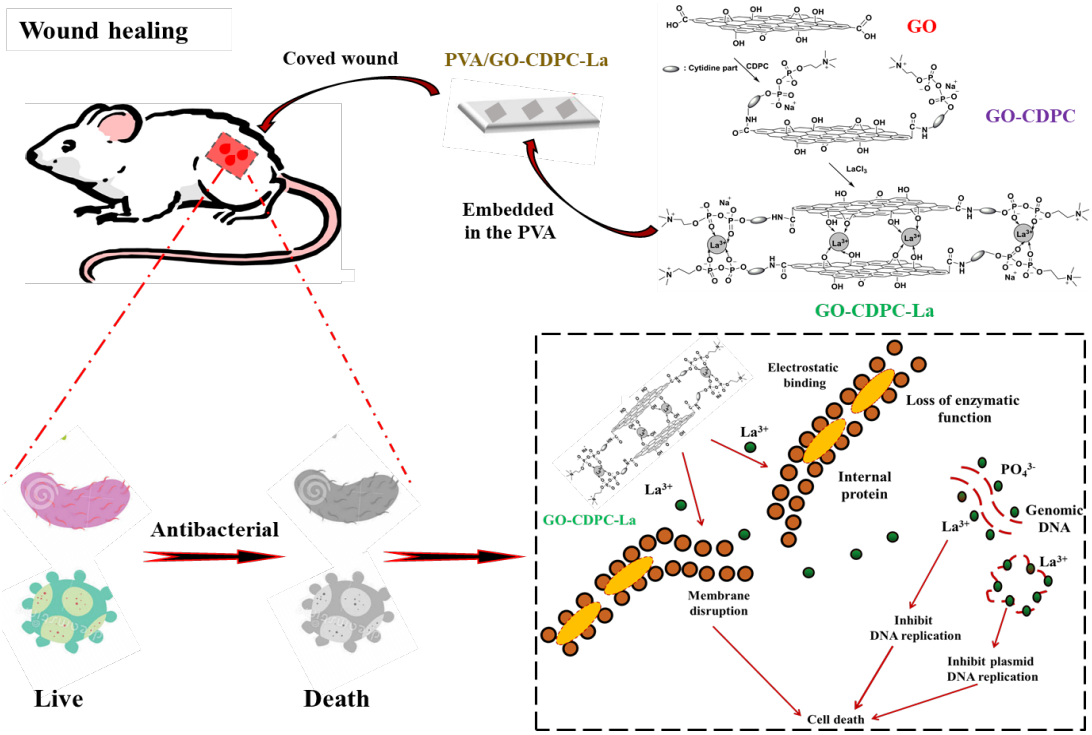

Fig. 1 Schematic illustration of PVA antibacterial film embedded with GO-CDPC-La for antibacterial wound dressings.

In this work, PVA/GO-CDPC-La films were prepared by complexing the prepared GO-CDPC-La and PVA by solution interaction (Fig. 1). When the mass ratio of GO: CDPC = 1:4, the highest number of CDPC molecules entered the GO layer through chemical bonding and adsorption. Therefore, GO-CDPC-La obtained in this ratio which was used to complex with PVA. In order to improve the hydrophilicity, antibacterial property and biocompatibility of PVA, the structure and property of PVA/GO-CDPC-La film was characterized by X-ray diffraction (XRD), thermogravimetric analysis (TGA), static contact angle (SCA), transmission electron microscopy (TEM), Scanning electron microscope (SEM), and X-ray photoelectron spectroscopy (XPS). The water absorption, protein adsorption capacity, cytotoxicity, and bacterial adhesion ability of the composites was studied to evaluate the biological properties. The effects of

PVA/GO-CDPC-La films on antibacterial activity was also investigated. An *in vivo* wound healing study was also conducted by using Wister rats.

2. Results and discussion

2.1. Characterization of GO-CDPC-La

The image of the shape characteristics of GO, GO-CDPC, and GO-CDPC-La was obtained by TEM. The GO before modification was mainly multilayer in the aqueous solution, the edges were wrinkled, and the sheet layers were not stretched completely (Fig. 2a). However, GO-CDPC could be dispersed completely, with slight wrinkles on the surface indicating the zwitterionic structure of CDPC could greatly improve the dispersibility of GO in aqueous solutions (Fig. 2b). The optimum mass ratios of GO and CDPC was determined by XRD and TGA, as shown in Fig. S1-S2. The feature of GO-CDPC-La changed significantly, the introduction of La^{3+} made the GO-CDPC sheet present a disordered shrinkage and aggregation in water (Fig. 2c). La^{3+} ions could interact with the oxygen-containing groups on the GO sheets and CDPC molecules connected to the surface, so that the cross-linking of GO-CDPC sheets can be achieved (Fig. 2d). The XRD was used to confirm the TEM results [32]. Compared with GO-CDPC, after adding $LaCl_3$, the diffraction peak of GO-CDPC at about 11.0° was significantly weaker (Fig. 2e), which indicated that during the preparation of GO-CDPC-La, the sheet of GO-CDPC further peeled off, and the initial orderly layered accumulation turned into disorder.

The thermal properties of GO-CDPC (1:4) and GO-CDPC-La were analyzed by the TGA curve [33]. Based on the TGA curve, the weight loss process of GO-CDPC and

GO-CDPC-La was divided into two stages. The first mass loss stage below 200 °C was induced by the evaporation of absorbed water (Fig. 2f), indicating the absorption capacity of water after GO-CDPC doping La^{3+} decreased. La^{3+} ions coordinated with oxygen atoms on the GO-CDPC, which reduced its ability to form hydrogen bonds with water molecules. GO-CDPC and GO-CDPC-La showed weight loss after 200 °C. In addition, the residual carbon ratio of GO-CDPC-La was higher than that of GO-CDPC. These changes indicated that a large amount of La^{3+} ions entered the GO-CDPC layer through electrostatic attraction and coordination, which reduced the content of organic matter per unit mass [34]. Besides, the formation of La-O coordination bonds delayed the decomposition of oxygen-containing functional groups and increased the heat stability of the GO-CDPC-La.

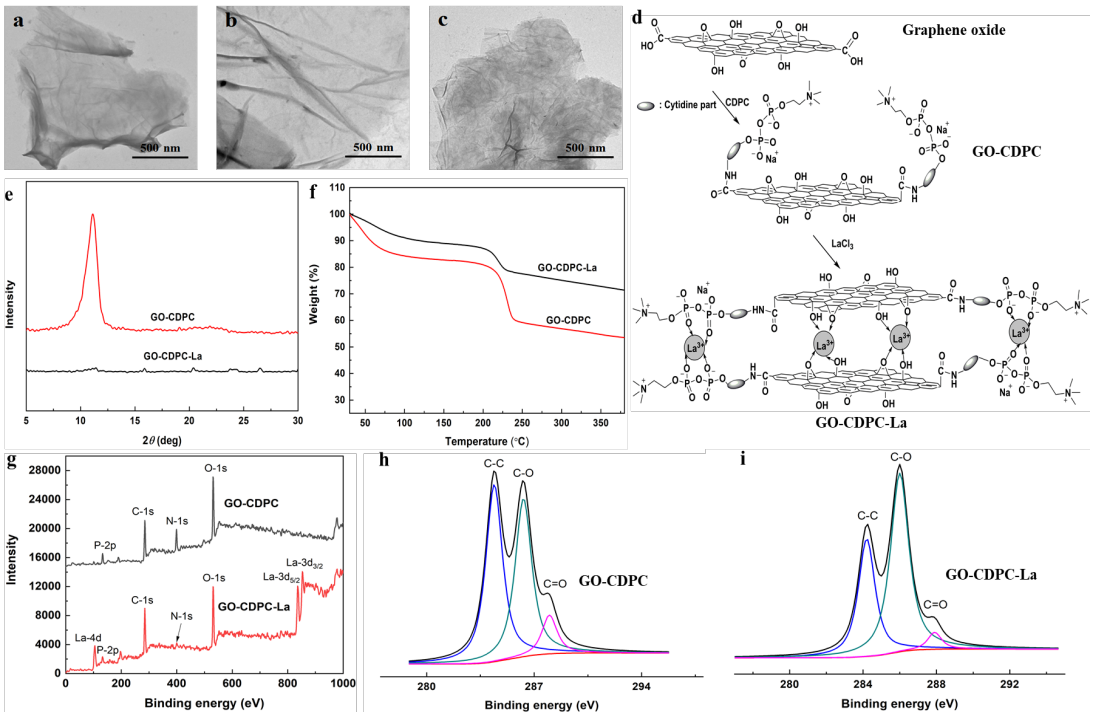

Figure. 2 (a) TEM of GO, (b) GO-CDPC (1:4) and (c) GO-CDPC-La. (d) Schematic illustration of the formation of GO-CDPC and GO-CDPC-La. (e) XRD curves of GO-CDPC and GO-CDPC-La.

(f) Weight loss curves of GO-CDPC and GO-CDPC-La. (g) XPS full scan and C1s narrow scan spectra of (h) GO-CDPC and (i) GO-CDPC-La.

XPS of GO-CDPC and GO-CDPC-La was used to characterize the functionalization of GO-CDPC. The XPS spectrum of GO-CDPC showed an absorption peak of element P at 132.3 eV (Fig. 2g), which proved that CDPC was successfully introduced. Meanwhile, the absorption peaks of La and C1 appeared in the spectrum of GO-CDPC-La. After the peak division of the C1s narrow sweep curve of GO-CDPC (Fig. 2h), the absorption at 284.4 eV, 286.3 eV, and 288.0 eV correspond to C-C, C-O, and C=O in GO-CDPC, respectively. Similarly, GO-CDPC-La exhibited characteristic absorptions of C-C, C-O, and C=O at 284.3 eV, 286.1 eV, and 287.9 eV (Fig. 2i). However, the ratio of the C-O bond peak area in GO-CDPC-La was obviously larger than that of the C-C bond, which might be caused by the breakage of the GO-CDPC sheet during the compounding of the GO-CDPC and La^{3+} ions.

2.2. Antimicrobial activity of GO-CDPC-La

Scientist observed the strong antimicrobial properties of GO and La^{3+} ions against a wide variety of both gram-positive and gram-negative bacterial pathogens. Physical and chemical interactions between GO and bacterial cells were the major causes for antimicrobial properties of GO [48]. In this process, the bacterial cell membrane was observed to be a primary target for cytotoxicity study of GO, the sharp edges of GO allowed it to penetrate through the cell membrane [49-50]. Because of the strong dispersion of GO and lipid molecules, a large number of phospholipids could be extracted from cell membrane. That was to say, GO degraded both the outer membrane

and the inner membrane of bacteria, causing the release of substances from the cell membrane [51]. Studies had shown that excessive release of certain biomolecules, such as Adenine and protein, could lead to the death of bacteria [52]. La^{3+} ions increased the permeability of cell membrane, which resulted in the release of biological factors such as Adenine and protein, which speeded up the death of bacteria. [53-54]. In addition, La^{3+} ions could bind to the phosphorus-oxygen bonds in bacterial DNA, preventing the DNA from replication, thereby killing bacteria [55-56].

The antimicrobial activities of the GO-CDPC-La were tested against a range of pathogenic and non-pathogenic micro-organisms, including Gram-negative bacteria (*E. coil*) and Gram-positive bacteria (*S. aureus*). With an increase in the concentration of GO-CDPC-La, the absorbance of the experimental group showed a certain downward trend, and the increase in the culture process was significantly lower than the blank group, indicating that the bacterial proliferation in the well plate was slow [35,36]. In particular, when the GO-CDPC-La concentration reached 2.0 mg/mL and 1.0 mg/mL, its absorbance remained unchanged in the first 8 h, indicating that GO-CDPC-La could almost completely inhibit *E. coli* and *S. aureus* at this time (Fig. 3a,b). In the middle and later stages of the culture, peaks corresponding to the absorptivity of the experimental group might appear, because the solvent evaporates, the GO-CDPC-La sediments and unevenly disperses at the bottom of the plate.

The efficacy of the anti-bacterial activity of GO-CDPC-La we prepared by minimum inhibitory concentration study was evaluated. For the two different strains, with an increase of GO-CDPC concentration, the absorbance showed an increasing

trend (Fig. 3c,d), because the higher concentration of GO-CDPC, and the greater influence of its own color on the absorbance of the solution [37]. However, it could still be seen that with an increase in the concentration to 1.0 mg/mL, the rate of increase in absorbance gradually weakened, or even decreased, indicating that with a high concentration of GO-CDPC, there was certain inhibitory effect on the growth of two bacteria, thus off-setting the increase in absorbance which is caused by the excessive color of GO-CDPC solution. For *E. coli* and *S. aureus*, when the GO-CDPC-La concentration reached 1.0 mg/mL, the absorbance reached the lowest level and stabilized, indicating that the growth of bacteria was basically inhibited at this time.

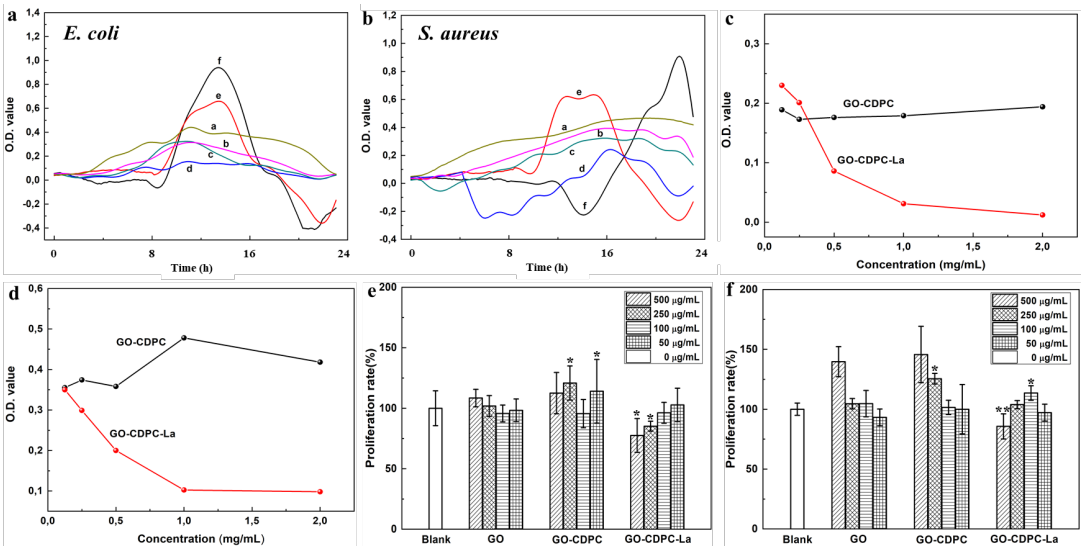

Fig. 3 (a) Inhibitory kinetic curves of GO-CDPC-La with the same amount of *E. coli* (a: 0 mg/mL, b: 0.125 mg/mL, c: 0.25 mg/mL, d: 0. 5 mg/mL, e: 1 mg/mL, and f: 2 mg/mL). (b) Inhibitory kinetic curves of GO-CDPC-La with *S. aureus* (a: 0 mg/mL, b: 0.125 mg/mL, c: 0.25 mg/mL, d: 0. 5 mg/mL, e: 1 mg/mL, and f: 2 mg/mL). (c) The Minimum inhibitory concentration curve of GO-CDPC and (d) GO-CDPC-La to *E. coli* and *S. aureus*. (e) The proliferation rate of GO, GO-CDPC, and GO-CDPC-La with 24 h (*$p < 0.05$ and **$p < 0.005$). (f) The proliferation rate of GO, GO-CDPC, and

GO-CDPC-La for 36 h (*p < 0.05).

2.3. In vitro cytotoxicity assays of GO-CDPC-La

Cytotoxicity is an important factor that determines the safety of biomedical material. *In vitro* cytotoxicity of various samples including GO, GO-CDPC, and GO-CDPC-La were investigated using NIH3T3 cells. The relative cell proliferation rate of GO-CDPC at different concentration gradients was more than 90% (Fig. 3e,f), the cytotoxicity was distributed at level 0 or 1, and the corresponding proliferation rate was higher than GO before modification because the CDPC molecule had the ability to repair cells and promoted their regeneration [38]. Due to the introduction of La^{3+}, the relative cell proliferation rate of GO-CDPC-La decreased slightly, but its cytotoxicity still did not exceed level 1 (Fig. S3). This result showed that both GO-CDPC and GO-CDPC-La had no obvious cytotoxicity and good biocompatibility, which could be used as biomedical materials.

2.4. Characterization of PVA/GO-CDPC-La (GO: CDPC= 1:4)

Fig. 4a displayed the SEM images of PVA/GO-CDPC-La film, the facture surface of pure PVA was smooth (Fig. S4), while the PVA/GO-CDPC-La film was rough, without any aggregation of GO, which confirmed the homogeneous dispersion of GO sheets in the PVA matrix [39]. Surface roughness was observed from the PVA/GO-CDPC-La film. The uniform distribution of GO-CDPC-La in the film was also confirmed by EDS elemental mapping as shown in Fig. S5. Fig. 4b and Table S1 showed the water contact angle on the surface of the PVA, PVA/GO-CDPC, and PVA/GO-CDPC-La film. The water contact angle of the PVA was 50.67° ± 0.94,

because the PVA had a large number of hydroxyl groups and good hydrophilicity. The addition of GO-CDPC and GO-CDPC-La further enriched the polar groups on the material surface, optimized the affinity of the PVA surface with water, and thus showed a smaller water contact angle, ensuring that the PVA/GO-CDPC-La film had the ability to keep the wound moist and reduce adhesion with wound tissue, which is a potential material for medical dressings. Furthermore, we compared the mechanical properties of pure PVA, PVA/GO-CDPC, and PVA/GO-CDPC-La film with a thickness of about 0.1 cm. As shown in Table S2, PVA/GO-CDPC-La film exhibited higher tensile strength than that of pure PVA. Similarly, there was an increase of 26% of the Young's modulus of the PVA-based film due to the incorporation of GO-CDPC-La.

The XRD pattern of PVA film showed weaker diffraction peaks around 2θ of 20 ° (Fig. 4c), which was generated by the semi-crystals in PVA film. However, the peak was weakened or even completely disappeared in PVA/GO-CDPC-La film. A large part of the generation of crystals in the PVA structure was due to the formation of hydrogen bonds between the hydroxyl groups on the molecular chains, allowing the molecular segments to be arranged tightly and neatly. After the addition of GO-CDPC and GO-CDPC-La, PVA entered the interlayer through the solution intercalation, and the oxygen-containing groups on the GO surface and the nucleotide sodium salt could form hydrogen bonds with PVA, which weakened the interaction between PVA chains, thereby changed the binding force and arrangement of macromolecular chains, increasing the disorder of material and making it difficult to form crystal structures [40]. Furthermore, the XRD curves of all composites did not show the characteristic peaks

of GO-CDPC-La at about 10°, indicating that the GO-CDPC-La was uniformly dispersed and exfoliated in the PVA matrix.

The thermal weight loss of PVA, PVA/GO-CDPC, and PVA/GO-CDPC-La film was conducted, as shown in Fig. 4d. The weight loss of PVA was mainly divided into three stages: the first stage, before 200 °C, was the volatilization of water molecules in the material; the second stage, from 200 °C to 350 °C, PVA removed adjacent hydroxyl groups to generate water, and then the cross-linked macromolecule's segment was broken, and the weight loss rate increases sharply; the third stage, from 350 ° C to 600 ° C, the PVA molecular chain continued to be carbonized. The weight loss rate of the PVA/GO-CDPC-La film in the second stage had increased to a certain extent, because the GO and nucleotide molecules also underwent thermal decomposition at this stage, and PVA matrix released small molecules together (Table S3). Nevertheless, the maximum weight loss temperature (T_{max2}) of the second stage of the PVA/GO-CDPC-La film had been shifted from the initial 255.7 °C to above 260 °C. Because the GO-CDPC-La sheet had certain heat insulation and oxygen barrier functionality, which delayed the decomposition of organic functional groups and the volatilization of small molecules. Furthermore, a certain amount of La^{3+} adsorbed on the surface of the sheet could be calcined to form La_2O_3 with high flame-retardant capacity, which optimized the thermal stability of the material. On the other hand, the residual carbon ratios of PVA, PVA/GO-CDPC, and PVA/GO-CDPC-La film was 0%, 1.32%, and 3.07%, respectively. The C framework made the residual carbon content of the material increase significantly. This result suggested that La^{3+} ions further improved the residual

quality of the material, which again showed that the addition of rare earth elements was beneficial to improve the thermal stability of PVA films.

The modified GO contained a large number of hydrophilic groups, such as hydroxyl groups, epoxy groups, and phosphate groups. The resulting composite material was more likely to form hydrogen-bonds with water molecules, thereby improving its wetting capabilities. The water absorption of La^{3+} ion containing composite material was lower than La^{3+} ion free composite materials (Table S4). This was because La^{3+} ions can also coordinate with the oxygen-containing groups in the modified GO and PVA molecular chains, which prevents further binding with water molecules. In general, PVA/modified GO nanocomposites had an impressive water absorption rate, which makes them useful in terms of their excellent ability to absorb wound exudate quickly and maintain wound moisturization.

2.5. Antimicrobial activity of PVA/GO-CDPC-La

For wound healing, the antibacterial properties of biomaterials are a major standard for defining an eligible wound dressing. To assess this ability, the antibacterial efficacy of PVA/GO-CDPC-La films against *E. coli* and *S. aureus* was measured (Fig. S6). The PVA film exhibited low antibacterial properties against both types of bacteria. However, the antibacterial properties of the PVA/GO-CDPC-La film were improved enormously. Furthermore, the SEM was used to observe the distribution of *E. coli* (Fig. 4e) and *S. aureus* (Fig. 4f) on the surface of the PVA, PVA/GO-CDPC, and PVA/GO-CDPC-La film [41]. It can be seen that more *E. coli* and *S. aureus* was distributed on the surface of the PVA film, and the structure was completed and the cells were full, indicating that

E. coli and *S. aureus* could normally adhere and reproduce on the surface of PVA. As the GO-CDPC optimized the hydrophilicity of the material surface, the number of *E. coli* cells adhered to the surface of PVA/GO-CDPC film decreased to a certain extent. The number of *E. coli* cells on the surface of the PVA/GO-CDPC-La film was significantly reduced. The absorption of La^{3+} in the GO-CDPC sheet could replace the binding site of Ca^{2+} in *E. coli* with a ion of similar ion radius, making the structure of lipopolysaccharide and peptidoglycan in the *E. coli* cell wall unstable and destroying the osmotic balance of the outer membrane of the cell causing a large amount of Ca^{2+} to be lost from the bacteria. Delightedly, the anti-adhesion ability of PVA/GO-CDPC-La films against *S. aureus* were significantly better than those for *E. coli*. Studies have shown that *S. aureus* needs to rely on extracellular nucleases to assist the hydrolysis reaction of phosphate diester bonds on DNA molecules [47]. The introduction of La^{3+} could not only damage its cell wall but also greatly inhibit the production and activity of nucleases, thus the overall activity of the bacteria was affected (Fig. 1).

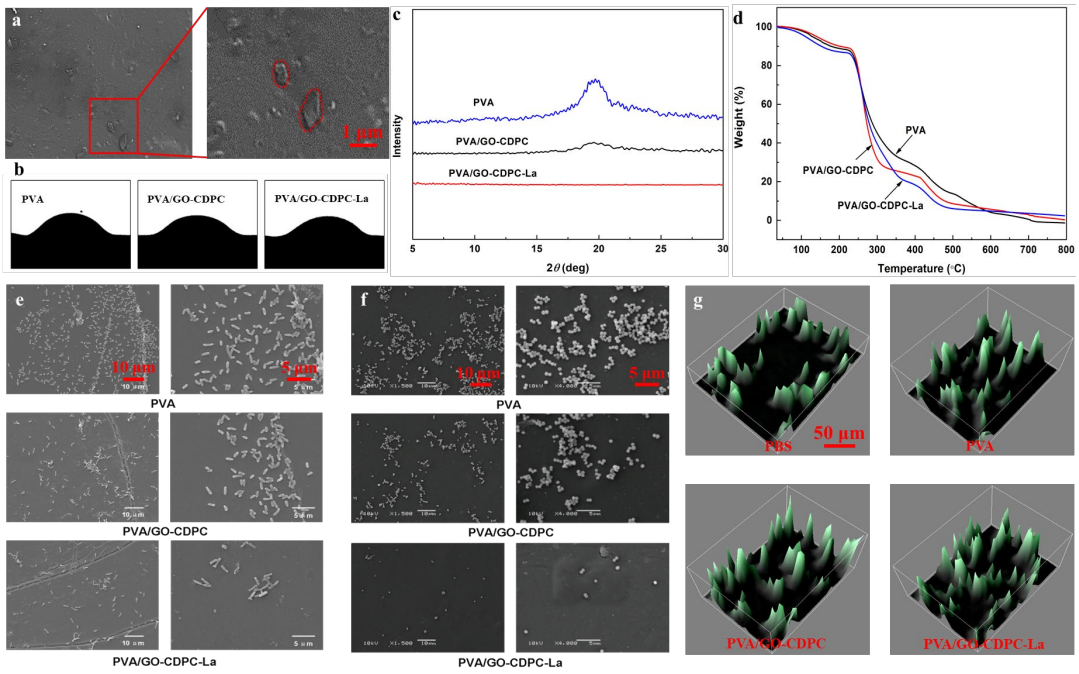

Fig. 4 (a) SEM images of PVA/GO-CDPC-La film. (b) SCA photographs of PVA, PVA/GO-CDPC, and PVA/GO-CDPC-La. (c) XRD curves of PVA, PVA/GO-CDPC, and PVA/GO-CDPC-La film. (d) Weight loss curves of PVA, PVA/GO-CDPC, and PVA/GO-CDPC-La film. (e) SEM images of *E. coli* exposed to PVA, PVA/GO-CDPC, and PVA/GO-CDPC-La film. (f) SEM images of *S. aureus* exposed to PVA, PVA/GO-CDPC, and PVA/GO-CDPC-La film. (g) CLSM images of PVA, PVA/GO-CDPC and PVA/GO-CDPC-La on the viability of live cell in the present of calcein-AM.

2.6. In vitro cytotoxicity assays

The effect of PVA, PVA/GO-CDPC, and PVA/GO-CDPC-La film on the viability of live cells was studied by laser scanning microscopy (CLSM) in the presence of calcein-AM (AM) staining (Fig. 4g). It should be noted that in AM, the AM stained live cells, appear as green in color. The results from the staining suggested that the green fluorescence was due to living cells, indicating an intact cell wall structure. Thus, PVA/GO-CDPC-La films showed no toxic effects.

2.7. Protein adsorption

The adsorption amount and type of proteins in living organisms on the surface of materials directly affected and even determined the way biomaterials interact with organisms [42]. Table S5 provided the data of protein adsorption per unit area of PVA, PVA/GO-CDPC, and PVA/GO-CDPC-La films calculated according to the standard curve of protein adsorption (Fig. S7). The protein adsorption capacity of PVA/GO-CDPC and PVA/GO-CDPC-La films had been improved to a certain extent, which was significantly different from blank PVA. Compared with PVA/GO-CDPC, the amount of protein absorbed by PVA/GO-CDPC-La increased more greatly. Corresponding to the PVA film with 0.05%, 0.1%, and 0.2% GO-CDPC-La, the amount of protein per unit area increased by 16.3%, 25.6%, and 24.1% respectively compared with PVA. La^{3+} in GO-CDPC-La had a stronger electrostatic attraction to the negatively charged bovine serum albumin, causing the surface of the material to absorb more protein.

2.8. Morphology of erythrocytes and coagulation test

After the red blood cells (RBCs) interacted with nanomaterials, its morphological change was a vital factor to evaluate the hemocompatibility of nanomaterials for bio-applications. RBCs presented fragmentation or aggregation indicating that incompatible nanomaterials interacted with RBCs [43]. The RBCs interacted with pure PBS which presented a normal circular shape (Fig. S8). In contrast, the RBCs contacted with PVA film showed a circular shape. The micrographs of RBCs incubated with PVA/GO-CDPC and PVA/GO-CDPC-La film retained the same circular morphology, indicating the samples did not influence on RBCs shape. To reveal the hemostatic

mechanism, the surface adhesion and morphologies of platelets on the PVA/GO-CDPC-La film was observed by SEM. Incubation with platelet-rich plasma (PRP) further demonstrated the platelet adhesion on the PVA, PVA/GO-CDPC, and PVA/GO-CDPC-La film surface. Compared with PVA films, larger platelet aggregated on PVA/GO-CDPC and PVA/GO-CDPC-La film (Fig. S9). These results also might indicated that the PVA/GO-CDPC-La film was helpful to improve the adsorption ability for platelets to achieve a rapid hemostatic effect.

2.9. NIH3T3 cells imaging on PVA/GO-CDPC-La

When a medical dressing comes into contact with damaged skin, proteins in the wound tissue fluid are immediately adsorbed on the surface of the material. The type and conformation of the protein adsorbed on the dressing surface directly determines the subsequent cell adsorption, migration, and proliferation [44]. The molecular chain of PVA could enter between the layers of GO-CDPC-La and form a crosslinked structure through hydrogen bonding. Furthermore, the GO-CDPC-La sheet could gradually migrate to the surface of the PVA film through the breakage and formation of hydrogen bonds. Existing research results showed that GO-CDPC-La and its derived materials could promote the adhesion and growth of a variety of cells, and the GO-CDPC-La on the surface of PVA could improve the compatibility of materials and cells to a certain extent, provide a more suitable environment for cell proliferation [31]. Fig. S10 showed the growth of NIH3T3 cells on the surface of blank PVA, PVA/GO-CDPC, and PVA/GO-CDPC-La film. It could be seen that NIH3T3 cells could grow normally and stably proliferate on the surface of PVA/GO-CDPC-La film, further illustrating that

PVA/GO-CDPC-La films had good biocompatibility and could promote wound healing [45].

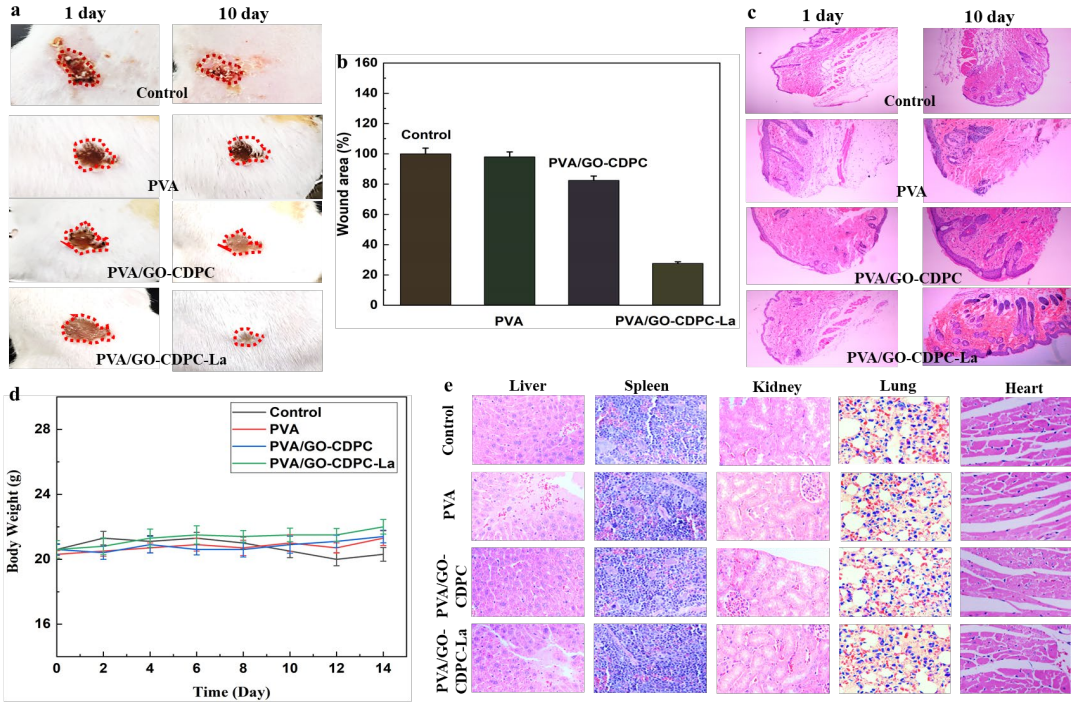

Fig. 5. (a) Photographs of wound treated with samples at days 1 and 10. (b) The wound area treated with samples at days 10. (c) The H&E images of the skin tissue samples on wounds after treating with samples at days 1 and 10. (d) The body weight of rat after treating with samples for 10 days. (e) The H&E images of the main organs after treating with samples at days 10.

2.10. In vivo antibacterial and healing efficacy of PVA/GO-CDOC-La

As metal ions, the safety of La^{3+} ions must be considered. La^{3+} ions entered the systemic circulation through the wound, but the absorption in the systemic circulation was extremely low and that absorbed drug was cleared predominantly by nonrenal mechanisms, which the main excretory pathway was hepatobiliary [57]. Low-level tissue deposition of lanthanum had been demonstrated in animals, primarily in bone (a natural sink for divalent and trivalent cationic metals) and liver (the main excretory

organ), but the experiment proved that La^{3+} ions had no toxic effect on bone cells [58]. In addition, La^{3+} ions had a low renal clearance, reducing the stress of kidney metabolism [59]. Thus, low dose La^{3+} had low toxicity and would not cause damage to human tissues [60-61].

The wound healing effect of PVA/GO-CDPC-La film was further evaluated in a full-thickness skin defect model. In Fig. 5a,b, the wound contraction of PVA, PVA/GO-CDPC, and PVA/GO-CDPC-La films were displayed on the 1^{st} and 10^{th} day. On the 10^{th} day, although the PVA/GO-CDPC and PVA/GO-CDPC-La films exhibited wounds with tiny diameters, the skin wounds healed better and faster after being treated with PVA/GO-CDPC-La film than with PVA/GO-CDPC film. Therefore, the result from PVA/GO-CDPC-La film demonstrated a better wound healing effect than PVA and PVA/GO-CDPC films, which was attributed to the combined effects of the inherent antibacterial and increased biocompatibility of CDPC, good chemical blocking and biocompatibility of PVA, and the excellent antibacterial effect of La^{3+}.

2.11. In vivo biocompatibility of PVA/GO-CDPC-La

Wound healing is a specific biological process that is comprised of the following phases: hemostasis, inflammation, migration, proliferation, and remodeling. Hematoxylin and eosin-stained sections (H&E) staining is employed to evaluate the wound healing progress in different phases [46]. All groups showed mild acute inflammatory responses on the first day, and there were numbers of inflammatory cells and fibroblasts migrating to the wound site (Fig. 5c). However, compared with PVA and PVA/GO-CDPC film groups, PVA/GO-CDPC-La film exhibited relatively less

inflammatory cells around the wound site, which attributed to antibacterial properties of La^{3+} that inhabit the inflammatory response around the wound area. When it came to the 10^{th} day, except for the formation of the basic structure of epithelium and dermis in control group, a few blood vessels and hair follicles were formed in the PVA/GO-CDPC-La film. These results demonstrated that the PVA/GO-CDPC-La film facilitated the wound healing process. In Fig. 5d, we measured the mice's body weight, as we expected, experiment and control mice did not show an obvious difference in body weight, and the mice did not show abnormality during the entire treatment period. Therefore, we determined that we used materials that had no obvious toxicity to the mice and had potential in clinical practice. Finally, the pathological image of major organs was demonstrated. Heart, liver, spleen, lung, and kidney were collected, sliced and stained by H&E (Fig. 5e). There was no apparent damage detected in all organs, especially in the liver, spleen, and kidneys.

3. Conclusions

In summary, we reported a therapeutic system for wound healing based on GO-CDPC-La, using PVA films as the carrier. GO-CDPC-La could be uniformly dispersed in the PVA matrix, while increasing the disorder of the PVA chain arrangement. Compared with blank PVA, the thermal stability of the PVA/GO-CDPC-La film was improved due to the thermal insulation and oxygen isolation capacity of GO-CDPC-La film. PVA/GO-CDPC-La films had good water absorption capacity and hydrophilicity, which could effectively absorb exudate from the wound, and kept the wound moist. Compared with blank PVA film, the protein adsorption on the surface of PVA/GO-

CDPC-La film was increased, because La^{3+} had stronger electrostatic attraction to bovine serum albumin. Importantly, the intrinsic properties of GO-CDPC-La allowed them to simultaneously fulfill the requirements of the excellent antibacterial activity, reusability, and biocompatibility. *In vivo* wound therapeutic outcomes which was realized effectively after GO-CDPC-La were loaded onto the PVA film. This work provided a simple, effective, and rapid strategy for wound disinfection by using PVA/GO-CDPC-La films.

Acknowledgments

This project was supported by the Foundation of Jiangsu collaborative innovation center of biomedical functional materials, the Jiangsu province science and technology support plan (BE2015367).

Conflicts of interest

The authors have no existing conflicts to declare.

References

[1] W. Yang, J.S. Owczarek, E. Fortunati, et al., Antioxidant and antibacterial lignin nanoparticles in polyvinyl alcohol/chitosan films for active packaging, Ind. Crops Prod. 94 (2016) 800-811.

[2] R.H. Xie, P.G. Ren, J. Hui, et al., Preparation and properties of graphene oxide-regenerated cellulose/polyvinyl alcohol hydrogel with pH-sensitive behavior, Carbohydr. Polym. 138 (2016) 222-228.

[3] E.Y. Yan, M.L. Cao, Y.W. Wang, et al., Gold nanorods contained polyvinyl alcohol/chitosan nanofiber matrix for cell imaging and drug delivery, Mater. Sci. Eng.: C 58 (2016) 1090-1097.

[4] M.T. Khorasani, A. Joorabloo, A. Moghaddam, et al., Incorporation of ZnO nanoparticles into

heparinised polyvinyl alcohol/chitosan hydrogels for wound dressing application, Int. J. Biol. Macromol. 114 (2018) 1203-1215.

[5] M. Jaiswal, K. Veena, K.D. Amit, In vitro and in vivo investigational studies of a nanocomposite-hydrogel-based dressing with a silver-coated chitosan wafer for full-thickness skin wounds, J. Appl. Polym. Sci. 133 (2016) 21.

[6] J. Qu, X. Zhao, Y. Liang, et al., Antibacterial adhesive injectable hydrogels with rapid self-healing, extensibility and compressibility as wound dressing for joints skin wound healing, Biomater. 183 (2018) 185-199.

[7] Y. Liang, X. Zhao, T. Hu, et al., Mussel-inspired, antibacterial, conductive, antioxidant, injectable composite hydrogel wound dressing to promote the regeneration of infected skin, J. Colloid Interface Sci. 556 (2019) 514-528.

[8] R.B. Trinca, C.B. Westin, J.A.F. Silva, et al., Electrospun multilayer chitosan scaffolds as potential wound dressings for skin lesions, Eur. Polym. J. 88 (2017) 161-170.

[9] B. Iqbal, N. Muhammad, A. Jamal, et al., An application of ionic liquid for preparation of homogeneous collagen and alginate hydrogels for skin dressing, J. Mol. Liq. 243 (2017) 720-725.

[10] S.S. Behera, U. Das, A. Kumar, et al., Chitosan/TiO2 composite membrane improves proliferation and survival of L929 fibroblast cells: Application in wound dressing and skin regeneration, Int. J. Biol. Macromol. 98 (2017) 329-340.

[11] F. Lotfipour, M. Alami-Milani, S. Salatin, et al., Freeze-thaw-induced cross-linked PVA/chitosan for oxytetracycline-loaded wound dressing: the experimental design and optimization, Res. Pharm. Sci. 14 (2019) 175-189.

[12] B. Chaudhuri, B. Mondal, S.K. Ray, et al., A novel biocompatible conducting polyvinyl alcohol (PVA)-polyvinylpyrrolidone (PVP)-hydroxyapatite (HAP) composite scaffolds for probable biological application, Colloids Surf., B 143 (2016) 71-80.

[13] N.T. Hiep, H.C. Khon, V.V.T Niem, et al., Microwave-assisted synthesis of chitosan/polyvinyl alcohol silver nanoparticles gel for wound dressing applications, Int. J. Polym. Sci. 2016 (2016).

[14] N.M. Aruan, I. Sriyanti, D. Edikresnha, et al., Polyvinyl alcohol/soursop leaves extract composite nanofibers synthesized using electrospinning technique and their potential as antibacterial wound dressing, Procedia Eng. 170 (2017) 31-35.

[15] P. Dubey, P. Gopinath, PEGylated graphene oxide-based nanocomposite-grafted chitosan/polyvinyl alcohol nanofiber as an advanced antibacterial wound dressing, RSC Adv. 6 (2016) 69103-69116.

[16] Q. Zhang, Q. Du, Y. Zhao, et al., Graphene oxide-modified electrospun polyvinyl alcohol nanofibrous scaffolds with potential as skin wound dressings, RSC Adv. 7 (2017) 28826-28836.

[17] N. Mohamad, E.Y.X. Loh, M.B. Fauzi, et al., In vivo evaluation of bacterial cellulose/acrylic acid wound dressing hydrogel containing keratinocytes and fibroblasts for burn wounds, Drug Delivery Transl. Res. 9 (2019) 444-452.

[18] S. Rossi, M. Mori, B. Vigani, et al., A novel dressing for the combined delivery of platelet lysate and vancomycin hydrochloride to chronic skin ulcers: Hyaluronic acid particles in alginate matrices, Eur. J. Pharm. Sci. 118 (2018) 87-95.

[19] X. Zhao, H. Wu, B. Guo, et al., Antibacterial anti-oxidant electroactive injectable hydrogel as self-healing wound dressing with hemostasis and adhesiveness for cutaneous wound healing, Biomater. 122 (2017) 34-47.

[20] A.A. Mahmoud, A.H. Salama, Norfloxacin-loaded collagen/chitosan scaffolds for skin reconstruction: Preparation, evaluation and in-vivo wound healing assessment, Eur. J. Pharm. Sci. 83 (2016) 155-165.

[21] R.H. Dong, Y.X. Jia, C.C. Qin, et al., In situ deposition of a personalized nanofibrous dressing via a handy electrospinning device for skin wound care, Nanoscale 8 (2016) 3482-3488.

[22] R. Belvedere, V. Bizzarro, L. Parente, et al., Effects of Prisma Skin dermal regeneration device containing glycosaminoglycans on human keratinocytes and fibroblasts, Cell Adhes. Migr. 12 (2018) 168-183.

[23] S. Kashyap, S.K. Pratihar, S.K. Behera, et al., Strong and ductile graphene oxide reinforced PVA nanocomposites, J. Alloy. Compd. 684 (2016) 254-260.

[24] Z.J. Fan, B. Lin, J.Q. Wang, et al., A novel wound dressing based on Ag/graphene polymer hydrogel: effectively kill bacteria and accelerate wound healing, Adv. Funct. Mater. 24 (2014) 3933-3943.

[25] F. Guo, H.Q. Zhang, G.S. Qiu, et al., Fabrication of LaCl3-containing nanofiber scaffolds and their application in skin wound healing, J. Appl. Polym. Sci. 135 (2018) 46672.

[26] J. Zhang, Z. Zhang, Y. Jiao, et al., The graphene/lanthanum oxide nanocomposites as electrode materials of supercapacitors, J. Power Sources 419 (2019) 99-105.

[27] Z.M. Geballe, H. Liu, A.K. Mishra, et al., Synthesis and stability of lanthanum superhydrides, Angew. Chem.-Int. Edit. 57 (2018) 688-692.

[28] J.W. Lu, Y. Miao, C.X. Guo, et al., Lanthanum-doped chitosan hydrogels promote the apoptosis of melanoma cells by Bcl-2/Bax pathway, ACS Appl. Bio Mater. 1 (2018) 1468-1477.

[29] Z. Lu, J.T. Gao, Q.F. He, et al., Enhanced antibacterial and wound healing activities of

microporous chitosan-Ag/ZnO composite dressing, Carbohydr. Polym. 156 (2017) 460-469.

[30] S. Niroomand, M.K. Motlagh, M. Noroozifar, et al, Photochemical and DFT studies on DNA-binding ability and antibacterial activity of lanthanum (III)-phenanthroline complex, J. Mol. Struct. 1130 (2017) 940-950.

[31] M. Zhang, W.T. Wang, P. Yuan, et al., Synthesis of lanthanum doped carbon dots for detection of mercury ion, multi-color imaging of cells and tissue, and bacteriostasis, Chem. Eng. J. 330 (2017) 1137-1147.

[32] W.T. Wang, T. Zheng, B.L. Sheng, et al., Functionalization of polyvinyl alcohol composite film wrapped in am-ZnO@CuO@Au nanoparticles for antibacterial application and wound healing, Appl. Mater. Today 17 (2019) 36-44.

[33] Y. Li, X.M. Liu, L. Tan, et al., Rapid sterilization and accelerated wound healing using Zn2+ and graphene oxide modified g-C3N4 under dual light irradiation, Adv. Funct. Mater. 28 (2018) 1800299.

[34] H. Tinwala, P. Shah, K. Siddhapara, et al., Investigation of ionic conductivity of lanthanum cerium oxide nano crystalline powder synthesized by co precipitation method, J. Cryst. Growth. 452 (2016) 54-56.

[35] M. Zhang, F. Wu, W.T. Wang, et al., Multifunctional nanocomposites for targeted, photothermal, and chemotherapy, Chem. Mater. 31 (2018) 1847-1859.

[36] Y. Yang, L. Ma, C. Cheng, et al., Nonchemotherapic and Robust Dual-Responsive Nanoagents with On-Demand Bacterial Trapping, Ablation, and Release for Efficient Wound Disinfection, Adv. Funct. Mater. 28 (2018) 1705708.

[37] M.A.M. Jahromi, P.S. Zangabad, S.M.M. Basri, et al., Nanomedicine and advanced

technologies for burns: Preventing infection and facilitating wound healing, Adv. Drug Delivery Rev. 123 (2018) 33-64.

[38] Y.W. Zhu, C. Xu, N. Zhang, et al., Polycationic Synergistic Antibacterial Agents with Multiple Functional Components for Efficient Anti-Infective Therapy, Adv. Funct. Mater. 28 (2018) 1706709.

[39] W. Tong, Y.H. Xiong, S. Duan, et al., Phthalocyanine functionalized poly (glycidyl methacrylate) nano-assemblies for photodynamic inactivation of bacteria, Biomater. Sci. 7 (2019) 1905-1918.

[40] J.F. Huang, J. Zhong, G.P. Chen, et al., A hydrogel-based hybrid theranostic contact lens for fungal keratitis, ACS nano, 10 (2016) 6464-6473.

[41] C.H. Yao, C.Y. Lee, C.H. Huang, et al., Novel bilayer wound dressing based on electrospun gelatin/keratin nanofibrous mats for skin wound repair, Mater. Sci. Eng. 79 (2017) 533-540.

[42] J. Qu, X. Zhao, Y.P. Liang, et al., Antibacterial adhesive injectable hydrogels with rapid self-healing, extensibility and compressibility as wound dressing for joints skin wound healing, Biomater. 183 (2018) 185-199.

[43] K. Yuan, B. Zhao, T. Cooper, et al., The management of degloving injuries of the limb with full thickness skin grafting using vacuum sealing drainage or traditional compression dressing: A comparative cohort study, J. Orthop. Sci. 24 (2019) 881-887.

[44] S. Bhakya, S. Muthukrishnan, M. Sukumaran, et al., Biogenic synthesis of silver nanoparticles and their antioxidant and antibacterial activity, Appl. Nanosci. 6 (2016) 755-766.

[45] C. Ergene, E.F. Palermo, Self-immolative polymers with potent and selective antibacterial activity by hydrophilic side chain grafting, J. Mater. Chem. B 6 (2018) 7217-7229.

[46] S.D. Huo, Y. Jiang, Z.W. Jiang, et al., Stable and oxidant responsive zwitterionic nanoclusters, Nanoscale 10 (2018) 7382-7386.

[47] R. Bomila, S. Srinivasan, S. Gunasekaran, et al., Enhanced photocatalytic degradation of methylene blue dye, opto-magnetic and antibacterial behaviour of pure and La-doped ZnO nanoparticles, J. Supercond. Nov. Magn. 31 (2018) 855-864.

[48] S. Gurunathan, J.W. Han, A.A. Dayem, et al., Oxidative stress-mediated antibacterial activity of graphene oxide and reduced graphene oxide in Pseudomonas aeruginosa, Int. J. Nanomed. 7 (2012) 5901–5914.

[49] L. Hui, J. Piao, J. Auletta, et al., Availability of the basal planes of graphene oxide determines whether it is antibacterial, ACS Appl. Mater. Interfaces 6 (2014) 13183–13190.

[50] S. Liu, M. Hu, T. Zeng, et al., Lateral dimension-dependent antibacterial activity of graphene oxide sheets, Langmuir 28 (2012) 12364–12372.

[51] Y. Tu, M. Lv, P. Xiu, et al., Destructive extraction of phospholipids from Escherichia coli membranes by graphene nanosheets, Nat. Nanotechnol. 8 (2013) 594–601.

[52] S.S. Nanda, D.K. Yi, K. Kim, Study of antibacterial mechanism of graphene oxide using Raman spectroscopy, Sci. Rep. 6 (2016) 1-12.

[53] P. Liu, H. Xiao, C. Zhang, et al., Study on the toxic mechanism of La^{3+} to Escherichia coli, Biol. Trace Elem. Res. 114 (2006) 293-299.

[54] P. Liu, Y. Liu, Z. Lu, et al., Study on biological effect of La^{3+} on Escherichia coli by atomic force microscopy, J. Inorg. Biochem. 98 (2004) 68−72.

[55] A. Hussain, D. Lahiri, M.S. Ameerunisha, et al., Photocytotoxic lanthanum (III) and gadolinium (III) complexes of phenanthroline bases showing light-induced DNA cleavage

activity, Inorg. Chem. 49 (2010) 4036-4045.

[56] Z. Wang, H. Lin, S. Zhu, et al., Spectroscopy, cytotoxicity and DNA-binding of the lanthanum (III) complex of an L-valine derivative of 1, 10-phenanthroline, J. Inorg. Biochem. 89 (2002) 97-106.

[57] M. Pennick, K. Michael, K. Dennis, S.J.P. Damment, Absolute bioavailability and disposition of lanthanum in healthy human subjects administered lanthanum carbonate, J. Clin. Pharmacol. 46 (2006) 738-746.

[58] G.J. Behets, G. Dams, S.R. Vercauternen, et al., Does the phosphate binder lanthanum carbonate affect bone in rats with chronic renal failure, J. Am. Soc. Nephrol. 15 (2004) 2219-2228.

[59] T. Shigematsu, Y. Takashi, et al., The management of hyperphosphatemia by lanthanum carbonate in chronic kidney disease patients, Int. J. Nephrol. Renovasc. Dis. 5 (2012) 81.

[60] H. Chen, S. Liu, L. Miao, et al., Inhibitory effect of lanthanum chloride on migration and invasion of cervical cancer cells, J. Rare Earths 31 (2013) 94-100.

[61] J. Lu, Y. Miao, C. Guo, et al., Lanthanum-Doped chitosan hydrogels promote the apoptosis of melanoma cells by Bcl-2/Bax pathway, ACS Appl. Bio Mater. 1 (2018) 1468−1477.